Quantum control of internal conversion in 24-vibrational-mode pyrazine

Cite as: J. Chem. Phys. **125**, 124310 (2006); https://doi.org/10.1063/1.2346684
Submitted: 10 July 2006 • Accepted: 07 August 2006 • Published Online: 28 September 2006

P. S. Christopher, M. Shapiro and P. Brumer

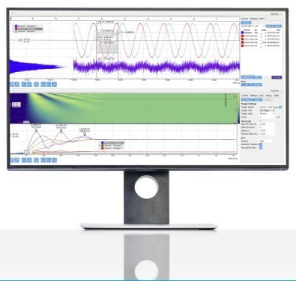

Quantum control of internal conversion in 24-vibrational-mode pyrazine

P. S. Christopher
Chemical Physics Theory Group, Department of Chemistry, University of Toronto, Toronto, Ontario M5S 3H6, Canada and Center for Quantum Information and Quantum Control, University of Toronto, Toronto, Ontario M5S 3H6, Canada

M. Shapiro
Department of Chemical Physics, The Weizmann Institute of Science, Rehovot 76100, Israel and Department of Chemistry, University of British Columbia, Vancouver, British Columbia V6T 1Z1, Canada

P. Brumer[a)]
Chemical Physics Theory Group, Department of Chemistry, University of Toronto, Toronto, Ontario M5S 3H6, Canada and Center for Quantum Information and Quantum Control, University of Toronto, Toronto, Ontario M5S 3H6, Canada

(Received 10 July 2006; accepted 7 August 2006; published online 28 September 2006)

Quantum control of the $S_2 \rightarrow S_1$ internal conversion in a complete 24-mode dimensionality model of pyrazine is demonstrated. The fully quantum mechanical study makes use of the recently developed "QP algorithm" for performing accurate computations of projected quantum dynamics and the role of overlapping resonances in control. The results are extremely encouraging, demonstrating *active* control over internal conversion so as to almost completely suppress the process over time scales of ~50–100 fs [well in excess of the natural internal conversion times (~20 fs)] or to accelerate it to complete internal conversion in less than 5 fs. A number of new diagnostics are introduced to demonstrate the significance of overlapping-resonance contributions to control. Control is far better than for a reduced dimensionality model of pyrazine, presumably because of the increased degree of overlap between bound state resonances existing in the full dimensionality case. © *2006 American Institute of Physics*. [DOI: 10.1063/1.2346684]

I. INTRODUCTION

The field of quantum control[1,2] deals with methods of utilizing quantum effects, and most often quantum interference effects, in the control of atomic and molecular processes. It is of great interest to develop a generic "toolbox," constituting a set of simple control scenarios, such as "interference between different quantum pathways" or " bichromatic control,"[1] "pump-dump" scenarios,[2] and adiabatic passage phenomena[3,4] displaying essential features of control. The hope is that all (numerically or experimentally derived) successful control endeavors would be shown to be composed of a sequence of such simple and understandable control scenarios. Only recently have experimental results been subjected to sufficient scrutiny[5–7] in search of these constituents. More work in this direction is anticipated.

Recently, a new tool has been added to the toolbox of generic control mechanisms, the "overlapping-resonance coherent control" scenario. Frishman and Shapiro[8] were the first to show that optimal control of the interference between overlapping resonances can be used to suppress spontaneous emission. This work was followed by Christopher *et al.* who illustrated the utility of the bound state analog of overlapping resonances in suppressing intermolecular "radiationless transitions" phenomena[10–16] and especially "internal conversion" (IC)—the radiationless electronic transitions between two excited singlet states—in model pyrazine.[17–22] Gerbasi *et al.*[23] have used similar ideas to control intermolecular vibrational redistribution processes with applications to model OCS.

In the present paper we reinvestigate the use of overlapping resonances to control internal conversion in pyrazine. It differs significantly from our earlier work in that, here, a substantially more realistic model of pyrazine, taking into account all 24 vibrational modes, is utilized. Our present treatment of all the vibrational modes is made possible by the development of a powerful new algorithm for the accurate calculation of projected quantum dynamics, the so-called QP algorithm.[24]

Internal conversion in pyrazine has been thoroughly studied theoretically and experimentally.[17–22] The process starts with the optical excitation from the ground vibrational state in S_0 (where S_0 is the ground electronic manifold) to the second electronically excited singlet state S_2. The optical excitation is then followed by a rapid IC process [lasting ~20 fs (Refs. 16 and 17)] to the first excited singlet state S_1.

There have been, to date, several physically motivated schemes to control IC in pyrazine.[9,25,26] Although the goal was the same, the means of controlling IC were distinctly different in each. Ferretti *et al.*[25] suggested controlling pyrazine using just the delay time between two very short light pulses. Sukharev and Seideman[26] have suggested suppressing IC in pyrazine by preferentially populating those eigenstates that happen to be predominately S_2 in character. Finally, Christopher *et al.*[9] have suggested a more general

[a)]Electronic mail: pbrumer@tikva.chem.utoronto.ca

scheme that relies upon preparing a particular initial superposition of molecular eigenstates so that one suppresses the IC process in the molecule by using interferences between the bound state analog of overlapping resonances.

The main limitation of the computations advocating the above control schemes has been their reliance on incomplete models of pyrazine that employ a significantly reduced number of vibrational modes,[9,25,26] usually 4 rather than 24. This was a result of the methodologies available at the time wherein calculations involving all 24 modes[17,27] were extremely time consuming and very demanding of storage space. Recently, the situation has been substantially improved by the introduction of our QP algorithm[24] that enables the study of large dimensionality radiationless transitions problems in reasonable computation times and use of reasonable storage space.

This paper makes use of the QP algorithm to demonstrate the viability of controlling IC in 24-mode pyrazine using the overlapping-resonances control scheme of Ref. 9. In doing so, we demonstrate the important result that the extent of control in the full 24-mode problem is substantially greater than that seen in the more limited, reduced dimensionality models. In addition, unphysical recurrences between electronic manifolds observed in the four-mode case are eliminated.

II. THEORY

A. Control using interference between overlapping resonances

Throughout this paper, and in keeping with our previous work[9,24] we refer to the manifold of vibrational states belonging to the S_1 electronic state as the P subspace and those belonging to the S_2 state as the Q subspace. The P-subspace basis states are denoted as $|\beta\rangle$ and the Q-subspace basis states as $|\kappa\rangle$. Thus, the projectors onto the P and Q subspaces are given as $P=\Sigma_\beta|\beta\rangle\langle\beta|$ and $Q=\Sigma_\kappa|\kappa\rangle\langle\kappa|$, respectively.

We consider using an incident laser pulse to prepare an initial (S_2) excited state,

$$|\psi(0)\rangle = \sum_\kappa c_\kappa|\kappa\rangle. \tag{1}$$

The radiationless evolution of this excited state is described as $|\psi(t)\rangle=U(t)|\psi(0)\rangle$, where $U(t)=e^{-iHt/\hbar}=\Sigma_\gamma|\gamma\rangle e^{-iE_\gamma t/\hbar}\langle\gamma|$ is the evolution operator, $|\gamma\rangle$ are the exact eigenstates of the molecule, and E_γ are the corresponding eigenvalues.

The amplitude of finding the system in the Q subspace at time t is given as $Q|\psi(t)\rangle$; hence the corresponding probability is given as

$$\mathcal{P}_Q(t) \equiv \langle\Psi(t)|Q|\Psi(t)\rangle = \sum_\kappa [c_\kappa]^2 g_\kappa(t) + \sum_{\kappa'\neq\kappa} c^*_{\kappa'} c_\kappa f_{\kappa'\kappa}(t), \tag{2}$$

where

$$g_\kappa(t) = \sum_{\kappa''} |\langle\kappa''|U(t)|\kappa\rangle|^2 = \sum_\gamma \sum_{\kappa''} |\langle k''|\gamma\rangle e^{-iE_\gamma t/\hbar}\langle\gamma|\kappa\rangle|^2,$$
$$f_{\kappa'\kappa}(t) = \sum_{\kappa''} \langle\kappa''|U(t)|\kappa'\rangle^*\langle\kappa''|U(t)|\kappa\rangle = \sum_{\gamma\gamma'} e^{-i(E_\gamma - E_{\gamma'})t/\hbar}\langle\kappa'|\gamma'\rangle\langle\gamma'|Q|\gamma\rangle\langle\gamma|\kappa\rangle. \tag{3}$$

Physically, the functions g_κ measure the dynamics of a system prepared in a single Q-subspace state $|\kappa\rangle$ [i.e., $|c_\kappa|=1$ implies that $\mathcal{P}_Q(t)=g_\kappa(t)$], while $f_{\kappa'\kappa}$ represent the dynamical interference between a pair of states $|\kappa\rangle$ and $|\kappa'\rangle$. The more $|\kappa\rangle$ and $|\kappa'\rangle$ interfere, the larger is the magnitude of $f_{\kappa'\kappa}(t)$. The fact that $f_{\kappa'\kappa}(t)$ represents interference makes it a quantity of central importance in coherent control and the overlapping-resonance mechanism.

It is important to note that the functions $g_\kappa(t)$ and $f_{\kappa'\kappa}(t)$ depend only on the properties of the material system; hence the effect of the controlling field is entirely contained in the preparation coefficients c_κ. Accordingly, the task of suppressing the IC process amounts to finding the set of c_κ coefficients that maximizes $\mathcal{P}_Q(T)$ at a desired "optimization time" T.

In order to better appreciate the concept of overlapping-resonances control, consider a superposition of only two basis states, i.e., we choose an initial superposition state given by $|\Phi\rangle=c_\kappa|\kappa\rangle+c_{\kappa'}|\kappa'\rangle$. It follows from Eq. (2) that $\mathcal{P}_Q(t)$ is in this case given as

$$\mathcal{P}_Q(t) = |c_\kappa|^2 g_\kappa(t) + |c_{\kappa'}|^2 g_{\kappa'}(t) + 2\,\mathrm{Re}[c_\kappa c^*_{\kappa'} f_{\kappa'\kappa}(t)]. \tag{4}$$

If $g_\kappa(T)\approx g_{\kappa'}(T)$, we have, due to the $\Sigma_\kappa|c_\kappa|^2=1$ normalization, that

$$\mathcal{P}_Q(T) \approx g_\kappa(T) + 2\,\mathrm{Re}[c_\kappa c^*_{\kappa'} f_{\kappa'\kappa}(T)]. \tag{5}$$

A direct result of this equation is that only the second term depends on the optimization variables c_κ, and controllability depends solely on the magnitude of $f_{\kappa'\kappa}(T)$. As a result, the degree of overlap between $|\kappa\rangle$ and $|\kappa'\rangle$ as measured by the product $\langle\kappa'|\gamma'\rangle\langle\gamma'|Q|\gamma\rangle\langle\gamma|\kappa\rangle$ plays an important role. Hence, determining the controllability of an overlapping-resonance case only requires knowledge of the $\langle\kappa|\gamma\rangle$ overlap integrals, an aspect of great utility.

The arguments above present the essence of the overlapping-resonance perspective, but some details are worth mentioning. First, frequently more than two states are involved in the superposition, constituting a straightforward extension of the above argument to multiple pairs of resonances. Second, the magnitude of $f_{\kappa\kappa'}$ depends not just on the overlap between the resonances of $|\kappa\rangle$ and $|\kappa'\rangle$ but also on any common overlap with a third state $|\kappa''\rangle$. In practice, this does not present a great complication, because generally the overlap of two basis states is a monotonically increasing function of the common third ket overlap (see below and Fig. 8). Finally, the paragraph above ignored the effect of the $\{g_\kappa(T)\}$ on the control by assuming that $g_\kappa(T)\approx g_{\kappa'}(T)$. This condition is not always met, as will be detailed below. It can

easily be seen from Eq. (4) that if $g_\kappa(T) > g_{\kappa'}(T)$, for instance, then $\mathcal{P}_Q(T)$ can be altered simply by changing the populations $|c_\kappa|^2$ and $|c_{\kappa'}|^2$. Further, if $g_\kappa(T)$ is significantly larger than $g_{\kappa'}(T)$, for example, then the maximized state would have $|c_\kappa| \approx 1$ and $|c_{\kappa'}| \approx 0$, a condition we have termed *passive control*[9] because it does not use quantum interferences between basis states to affect control.

Understanding the passive or active nature of a control scenario is important for understanding the underlying mechanism. We therefore explore this issue in greater detail. Equation (4) can be written as

$$\mathcal{P}_Q(T) = |c_\kappa|^2 g_\kappa(T) + |c_{\kappa'}|^2 g_{\kappa'}(T) + 2|c_\kappa||c_{\kappa'}| \times |f_{\kappa'\kappa}(T)| \cos(\chi + \phi), \tag{6}$$

where χ is the phase difference between c_κ and $c_{\kappa'}$ and ϕ is the phase of $f_{\kappa'\kappa}$. It follows then that if $g_\kappa(T) = g_{\kappa'}(T)$, $\mathcal{P}_Q(T)$ attains its extremal values when $|c_{\kappa'}| = |c_\kappa| = 2^{-1/2}$, with the maximum achieved at $\chi + \phi = 0$ and the minimum at $\chi + \phi = \pi$.

To quantify the extent of control we define the degree of controllability $\mathcal{L}$ as

$$\mathcal{L}(T) = \mathcal{P}_Q^{(\max)}(T) - \mathcal{P}_Q^{(\min)}(T), \tag{7}$$

where $\mathcal{P}_Q^{(\max)}(T)$ [or $\mathcal{P}_Q^{(\min)}(T)$] denotes the maximal (or minimal) $\mathcal{P}_Q$ at the target time T. It is readily seen from Eq. (6) that if $g_\kappa(T) \approx g_{\kappa'}(T)$, leading to $|c_{\kappa'}^{(\max)}| = |c_\kappa^{(\max)}| = 2^{-1/2}$, then $\mathcal{L}$ is given by $2|f_{\kappa'\kappa}|$. On the other hand, if $g_\kappa(T) > g_{\kappa'}(T)$ and control is completely passive, i.e., $|c_\kappa^{(\max)}| = 1$, $|c_{\kappa'}^{(\max)}| = 0$ and $|c_\kappa^{(\min)}| = 0$, $|c_{\kappa'}^{(\min)}| = 1$, then the controllability is $\mathcal{L} = |g_\kappa(T) - g_{\kappa'}(T)|$. Hence $c_\kappa^{(\max)}$ and $c_\kappa^{(\min)}$ denote the values of the coefficients associated with maximization or minimization of $\mathcal{P}_Q$.

The above discussion leads one to the conclusion that the active or passive nature of the control can be measured by calculating

$$R_{\kappa'\kappa} = \frac{2|f_{\kappa'\kappa}|}{2|f_{\kappa'\kappa}| + |g_\kappa - g_{\kappa'}|} \tag{8}$$

and $\sigma_{\kappa'\kappa}$, "the degree of passivity" of the control, given as

$$\sigma_{\kappa'\kappa} = ||c_\kappa^{(\max)}|^2 - |c_\kappa^{(\min)}|^2| = ||c_{\kappa'}^{(\max)}|^2 - |c_{\kappa'}^{(\min)}|^2|. \tag{9}$$

As can be verified from the above discussion, $\sigma_{\kappa'\kappa} = 1$ for completely passive control and $\sigma_{\kappa'\kappa} = 0$ for completely active control. When the number of states used in the optimization is larger than 2, $\sigma_{\kappa\kappa'}$ is no longer useful as a measure of the passivity of the optimized state. Rather, a new measure of passivity is needed and we define the degree of interference $D_c(t)$ as

$$D_c(t) = \sum_{\kappa \neq \kappa'} c_\kappa c_{\kappa'}^* f_{\kappa\kappa'}(t). \tag{10}$$

This is simply the second sum of the right hand side of Eq. (2) and measures the contribution of interference to the system dynamics.

Finally, a few additional definitions will prove useful. We define two measures of the overlap of two resonances:

$$\Omega_{\kappa\kappa'} = \sum_\gamma |\langle\kappa|\gamma\rangle||\langle\gamma|\kappa'\rangle| \tag{11}$$

and

$$A_{\kappa\kappa'} = \sum_{\kappa''} \Omega_{\kappa\kappa''}\Omega_{\kappa''\kappa'}. \tag{12}$$

$\Omega_{\kappa\kappa'}$ is an intuitive measure of the overlap of two resonance shapes, and $A_{\kappa\kappa'}$ is designed to expose the common third state overlap between $|\kappa\rangle$ and $|\kappa'\rangle$. That is, the criteria for active control are either overlap between the two resonances or their overlap with a common third state. The relationship between $\Omega_{\kappa\kappa'}$ and $A_{\kappa\kappa'}$ is explored below.

B. Pyrazine dynamics and optimization

In the first stage of the computation, we used the QP algorithm[24] to calculate the eigenstates and eigenvalues of the 24-mode model of pyrazine of Raab *et al.*[17] This model expresses the vibrational motion of pyrazine in terms of a set of oscillators, described by the (dimensionless) normal coordinates Q_i coupled by linear and quadratic functions of Q_i. The S_1 plus S_2 Hamiltonian is given as

$$H = \sum_i \begin{pmatrix} 1 & 0 \\ 0 & 1 \end{pmatrix} \frac{\omega_i}{2}\left(\frac{\partial^2}{\partial Q_i^2} + Q_i^2\right) + \begin{pmatrix} -\Delta & 0 \\ 0 & \Delta \end{pmatrix} + \sum_{i \in G_1} \begin{pmatrix} a_i & 0 \\ 0 & b_i \end{pmatrix} Q_i + \sum_{i,j \in G_2} \begin{pmatrix} a_{ij} & 0 \\ 0 & b_{ij} \end{pmatrix} Q_i Q_j + \begin{pmatrix} 0 & \lambda_{10a} \\ \lambda_{10a} & 0 \end{pmatrix} Q_{10a} + \sum_{i,j \in G_4} \begin{pmatrix} 0 & c_{ij} \\ c_{ij} & 0 \end{pmatrix} Q_i Q_j. \tag{13}$$

Here ω_i are the normal mode frequencies of the lowest states of S_0, 2Δ is the energy difference between the zero points of the S_2 and S_1 potential energy surfaces, a_i, b_i, a_{ij}, and b_{ij} are "intrasurface" coupling constants, and λ_{10a} and c_{ij} are "intersurface" coupling constants. These constants were determined by fitting the above functional form to the *ab initio* derived points on the potential energy surface. The linear couplings only occur within the A_g symmetry set of modes, denoted as G_1. The quadratic couplings occur between the set of modes whose products are either of A_g symmetry, denoted as G_2, or of B_{1g} symmetry, denoted as G_4.

As mentioned above, our strategy is to first compute the system eigenstates and eigenvalues using the QP algorithm. In fact, the QP algorithm is the only method currently available that can be used to optimize the 24-mode pyrazine dynamics. Wave packet propagations, by e.g., the multiconfigurational time dependent Hartree (MCTDH) method[17] or semiclassical methods,[27] cannot be used for the optimization problem because with these methods, each set of preparation coefficients requires repeating anew the entire time dependent propagation. In view of the enormous effort involved in each 24-mode wave packet propagation calculation, optimization of the input pulse, which may require hundreds of

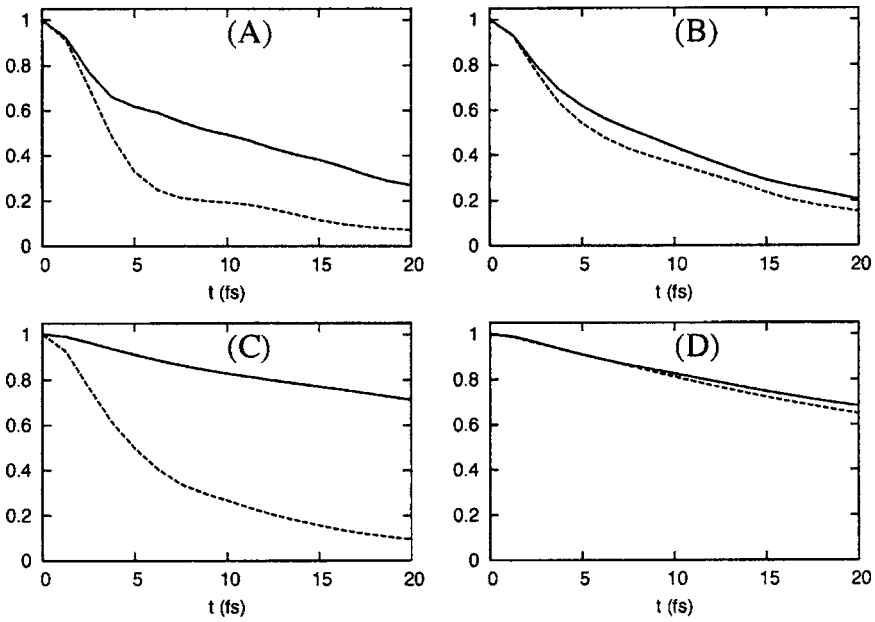

FIG. 1. Maximized and minimized $P_2(t)$ vs time using (a) resonances at 0.68 and 0.60 eV ($\Omega_{\kappa'\kappa}$=0.7), (b) resonances at 1.04 and 0.83 eV ($\Omega_{\kappa'\kappa}$=0.3), (c) resonances at 0.96 and 0.94 eV ($\Omega_{\kappa'\kappa}$=0.3), and (d) resonances at 0.916 and 0.913 eV ($\Omega_{\kappa'\kappa}$=0.72).

runs, would be entirely out of the question. By contrast, in the QP method we solve once for the eigenstates and (coarse grained) eigenvalues (a task requiring 40 min. when distributed over forty 1.8 GHz AMD Opteron processors in a vanilla Beowulf configuration). The eigenstates and eigenvalues, once obtained, can be effortlessly used over and over again to optimize the time dependent dynamics.

The number of S_2 states included in the Q subspace was chosen to be 176. This number was found to be sufficiently large to represent the dynamics accurately, a fact verified by comparisons with the computations of Thoss *et al.*[27] for the Raab Hamiltonian, yet to be sufficiently small to make the computations relatively inexpensive. Further details of the QP algorithm and its use for the case of pyrazine IC dynamics are provided in Ref. 24.

The optimization of the IC process proceeds as follows: Given a vector of c_κ preparation coefficients, denoted as $\underline{\mathbf{c}}$, Eq. (2) may be written as[8,9]

$$\mathcal{P}_Q(t) = \underline{\mathbf{c}}^\dagger \cdot \underline{\underline{\mathbf{K}}}(t) \cdot \underline{\mathbf{c}}, \tag{14}$$

where † denotes the Hermitian adjoint, and the matrix $\underline{\underline{\mathbf{K}}}(t)$ is given as

$$K_{\kappa'\kappa} \equiv g_\kappa \delta_{\kappa'\kappa} + f_{\kappa'\kappa}(1 - \delta_{\kappa'\kappa}), \tag{15}$$

with g_κ and $f_{\kappa'\kappa}$ being defined in Eq. (3). It is easy to see[8,9] that maximization of $\mathcal{P}_Q(T)$ of Eq. (14), subject to the $\mathbf{c}^\dagger \cdot \underline{\mathbf{c}} = 1$ constraint, results in the eigenvalue equation

$$\underline{\underline{\mathbf{K}}}(T) \cdot \underline{\mathbf{c}}^{(\max)} = \lambda^{(\max)}(T)\underline{\mathbf{c}}^{(\max)}. \tag{16}$$

A similar equation holds for $\underline{\mathbf{c}}^{(\min)}$ and $\lambda^{(\min)}(T)$.

III. RESULTS

Because IC in pyrazine comprises the transfer of population from the S_2 manifold to the S_1 manifold, the *suppression* of the IC process is attained by maximizing $P_2(t) \equiv \mathcal{P}_Q(t)$, the probability of observing the molecule in the S_2

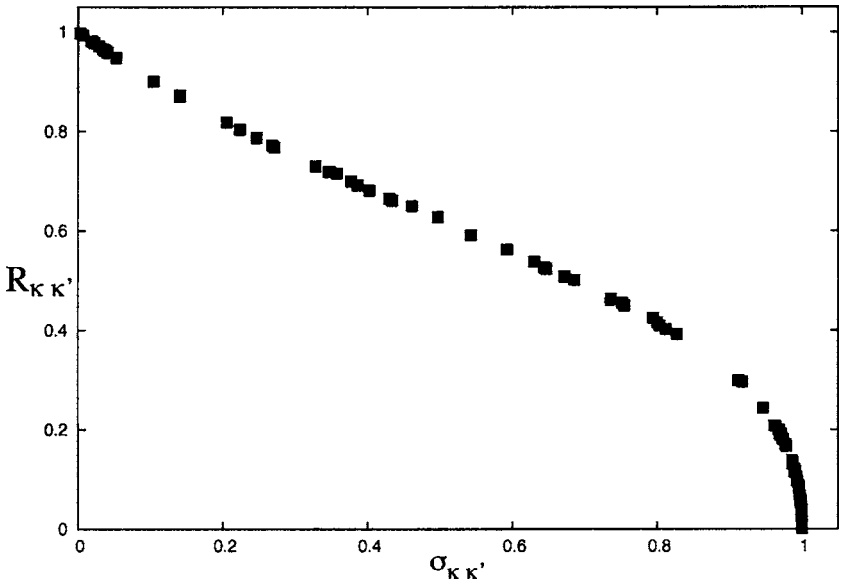

FIG. 2. $R_{\kappa\kappa'}$ vs $\sigma_{\kappa\kappa'}$ for a representative selection of resonance pairs.

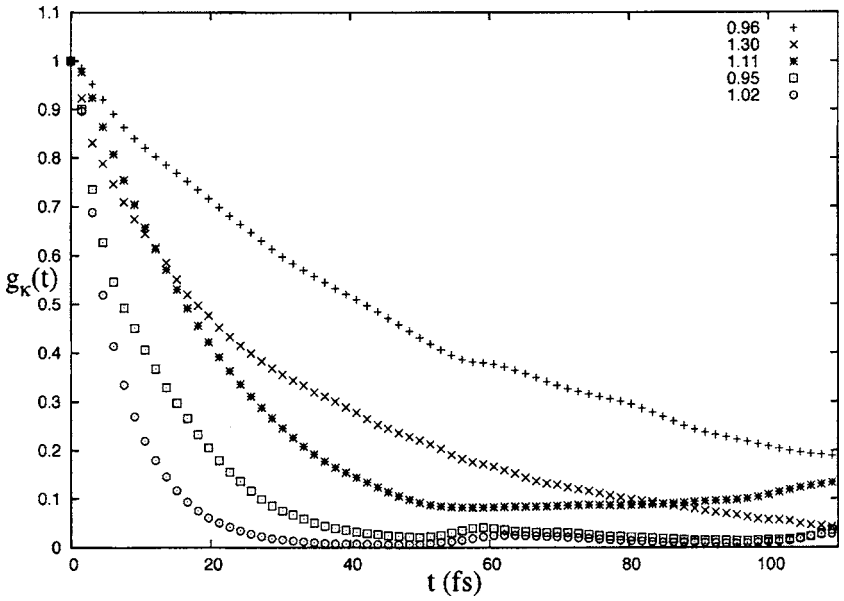

FIG. 3. g_κ for several resonances. Most resonances of our basis have g_κ curves that are bracketed by the 1.11 eV curve from above and the 1.02 eV curve from below.

subspace. Likewise, the *enhancement* of the IC process is attained by minimizing $P_2(t)$. As explained above, we perform the optimization at a specific target time $t=T$, anticipating, as indeed happens, that the desired goal(s) is (are) also met at neighboring times.

Consider first the use of just two overlapping resonances. Figure 1(a) shows $P_2^{(\max)}(t)$ and $P_2^{(\min)}(t)$ for a pair of states that can be actively controlled due to their strong resonance overlap ($\Omega_{\kappa'\kappa}=0.7$). The optimization target time $t=T$ was chosen here to be 10 fs, but as is evident in the figure, the effect of optimization is seen at other times as well. Even though there are only two coefficients to optimize, we see an extensive range of control.

Figure 1(b) shows the same plots for two states of only moderate overlap ($\Omega_{\kappa'\kappa}=0.3$). Clearly, the controllability here is greatly diminished relative to the first case. Consistent with this result, we find that the *passivity* of the control of Fig. 1(b) ($\sigma_{\kappa'\kappa}=0.75$) is greater than that of Fig. 1(a) ($\sigma_{\kappa'\kappa}=0.14$).

The above data are in keeping with a general trend for two states control; states with fixed $|g_\kappa(t)-g_{\kappa'}(t)|$ tend to be more controllable, and in a more active fashion, as the degree of mutual overlap $\Omega_{\kappa'\kappa}$ increases. This is because an increase in $\Omega_{\kappa'\kappa}$ is accompanied by an increase in $f_{\kappa'\kappa}(T)$, thereby increasing the $R_{\kappa'\kappa}$ ratio of Eq. (8). This point is illustrated in Fig. 2 where we plot $R_{\kappa'\kappa}$ versus the passivity $\sigma_{\kappa'\kappa}$ for a series of randomly selected pairs of states optimized at 10, 20, and 30 fs. Clearly from this figure and from Eq. (8), as $f_{\kappa'\kappa}$ increases in magnitude compared to $|g_\kappa-g_{\kappa'}|$, the nature of the control becomes more and more active.

There are, however, instances where our results appear to differ from the trend identified above. In Fig. 1(c) we display an impressive range of control for a pair of states that have only moderate overlap, $\Omega_{\kappa'\kappa}=0.3$. In this case the magnitude of $|g_\kappa(T)-g_{\kappa'}(T)|$ is large. As a result the control is primarily passive with $\sigma_{\kappa'\kappa}\approx 1$, though the controllability is large because it is equal to $\mathcal{L}=|g_\kappa(T)-g_{\kappa'}(T)|$.

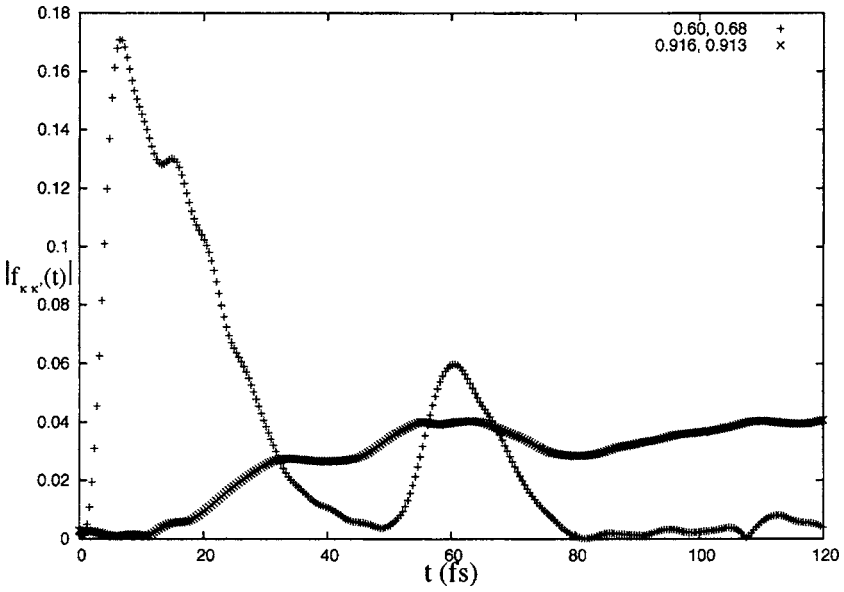

FIG. 4. $|f_{\kappa\kappa'}|$ vs time for the resonances used in Figs. 1(a) (0.60, 0.68) and 1(d) (0.916, 0.913).

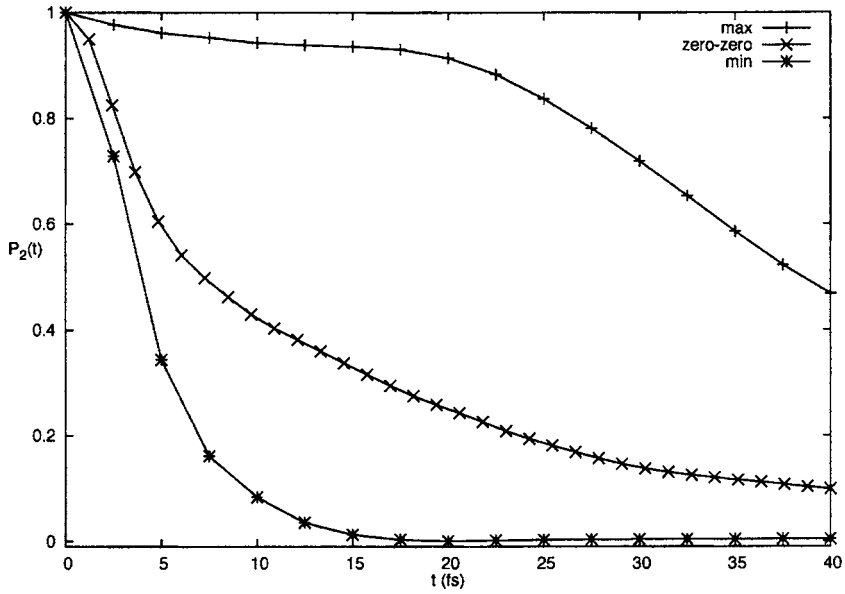

FIG. 5. Maximized and minimized $P_2(t)$ vs time for a set of 176 resonances with optimization time of 20 fs. Also shown for reference is the $P_2(t)$ for the zero-zero state (described in the text).

In Fig. 3, we display $g_\kappa(t)$ for a representative set of zero-order S_2 energies. Although $g_\kappa(t)$ and its time dependence appear to vary considerably, in fact, the time dependence of most of the $|\kappa\rangle$ states appears to be well bracketed by the $g_{1.11\ \mathrm{eV}}$ curve from above and by the $g_{1.02\ \mathrm{eV}}$ curve from below. As a result of this similarity between a large group of decay curves, the situation is well described by Eq. (5), and as pointed out above, when this happens, controllability depends solely on the magnitude of $f_{\kappa'\kappa}(T)$ and on the degree of overlap between resonances.

In support of this analysis, we show in Fig. 1(d) a case in which $P_2^{(\max)}(t)$ is very similar to $P_2^{(\min)}(t)$ for a pair of well overlapping resonances, $\Omega_{\kappa'\kappa}=0.72$. The results can be contrasted with those in Fig. 1(a). In the former case, controllability is small because $|f_{\kappa'\kappa}(T)|$ happens to be small at the particular optimization time, e.g., at 10 fs. To see this, consider Fig. 4, where $|f_{\kappa'\kappa}(t)|$ is presented for the two pairs of states in Figs. 1(a) and Fig. 1(d). The $|f_{\kappa'\kappa}(t)|$ curve with the large peak around 6 fs corresponds to the 0.68, 0.60 eV pair, whose extensive control is shown in Fig. 1(a). By contrast, the other curve (corresponding to the 0.916, 0.913 eV pair) pertains to the pair of states pictured in Fig. 1(d). Clearly, $|f_{\kappa'\kappa}(t)|$ is much larger at the 10 fs optimization time for the 0.68, 0.60 eV pair than for the 0.916, 0.913 eV pair; hence control is far better for the former pair of states. Note also that due to the different time variation of $|f_{\kappa'\kappa}(t)|$ for different pairs, optimizing at other target times can completely change the extent of control.

The main goal of the preceding discussion was to highlight the role of good overlap between pairs of resonances and to extract a set of rules for control using pairs of states. As noted above, there are exceptions to these rules, but we expect these exceptions to become less noticeable as more states are used in the IC control. This can be understood by recognizing that the number of terms in the second term on the right hand side of Eq. (2) [or equivalently the degree of interference $D_c(t)$] increases rapidly as the number of states increases.

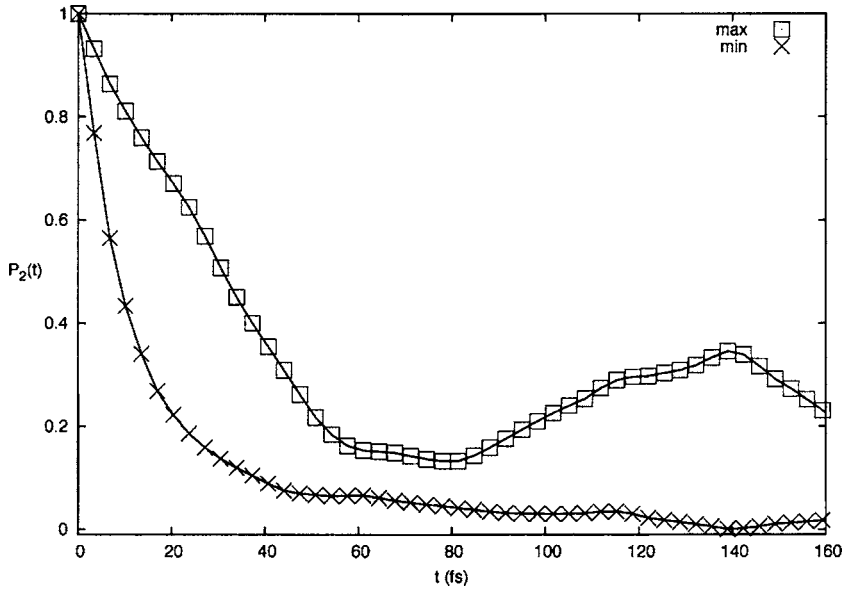

FIG. 6. Maximized and minimized $P_2(t)$ vs time for a set of 176 resonances with optimization time of 140 fs.

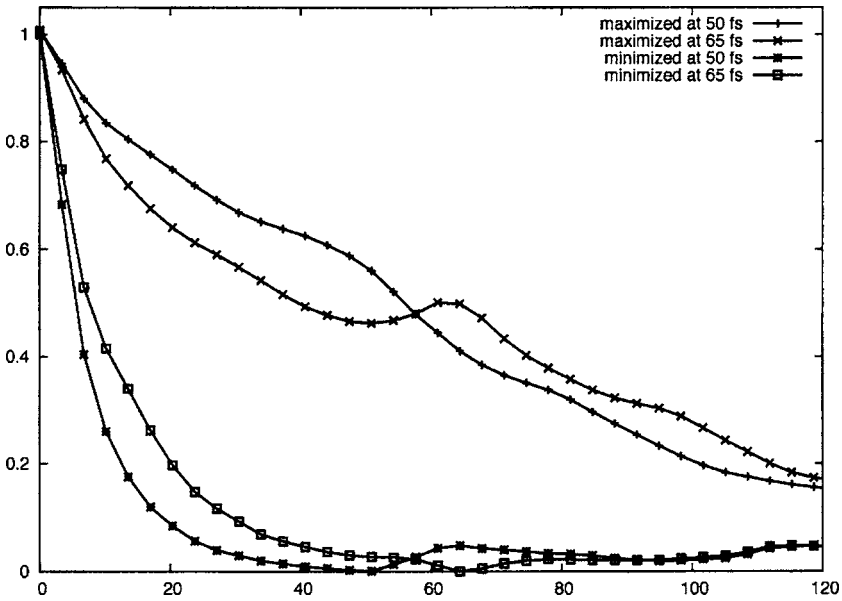

FIG. 7. Maximized and minimized $P_2(t)$ vs time for a set of 176 resonances with optimization time of 50 and 65 fs. Notice that the recrossing hump appears for the optimization at 65 fs.

Consider then the multiresonance control. Figure 5 shows the $P_2(t)$ curves for both the maximized and minimized initial states where all 176 Q-subspace basis states are included in the optimization. For reference we also include the decay of the zero-zero state, where the zero-zero state is the ground vibrational state of S_0 projected onto the S_2 manifold. We first note that this figure shows impressive controllability, by far exceeding that observed using just a pair of states; we attain $P_2^{(\max)}(T)>0.9$ and $P_2^{(\min)}(T)<10^{-4}$, with the corresponding controllability $\mathcal{L}$ exceeding 0.9. Significantly, this controllability also substantially exceeds that observed in our past, reduced dimensionality studies.[9]

As mentioned above, the large multiresonance effect is due to the increase of the interference contribution $D_c(T)$ as the number of resonances is increased. Typically in the multiresonance case, $D_c(T)=0.3$ and $D_c(T)=0.14$ for the maximized and minimized curves, respectively, whereas a typical value of $D_c(T)$ for a single pair of resonances is of the order of 0.06. A further example of the important effect of interstate interference can be seen by comparing the various functions in Fig. 3 with the decays of Fig. 5. The important point is that the maximized (minimized) decay curve of Fig. 5 is greater (less) than any of the g functions of Fig. 3 by a significant amount.

Control is not limited to just short times. Figure 6 shows the decay of $P_2(t)$ for initial states maximized or minimized at 140 fs. We see, similar to the 20 fs calculation of Fig. 5, that the range of control in this case is good, with $P_2^{(\max)}\times(T)>0.34$ and $P_2^{(\min)}(T)<10^{-3}$. As in Fig. 5, the maximized state of Fig. 6 experiences a larger degree of interference compared to pairs of states, with $D(T)$ being 0.21 and 0.034 for the maximized and minimized curves, respectively.

One of the most striking features of Fig. 6 is the strong recurrence of $P_2^{(\max)}(t)$ around the target optimization time, as seen by the peak at $\sim$140 fs. This interesting feature indicates that after flowing from the Q subspace into the P subspace, a substantial part of the wave packet finds its way

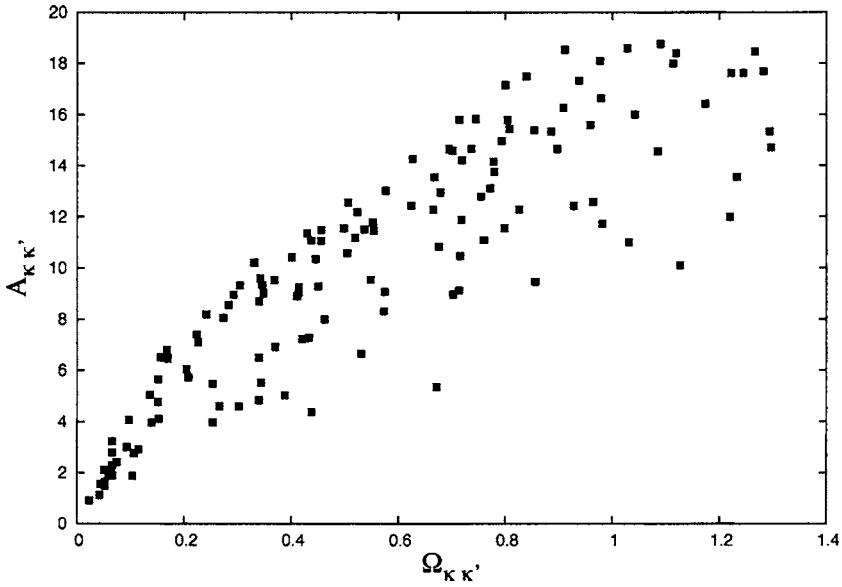

FIG. 8. $A_{\kappa\kappa'}$ vs $\Omega_{\kappa\kappa'}$ for a selection of representative resonance pairs. Notice that, because $A_{\kappa\kappa'}$ is monotonic with $\Omega_{\kappa\kappa'}$, overlap between two resonances and their common third resonance overlap are highly correlated. This means that the overlap of two resonances is a key indicator of controllability.

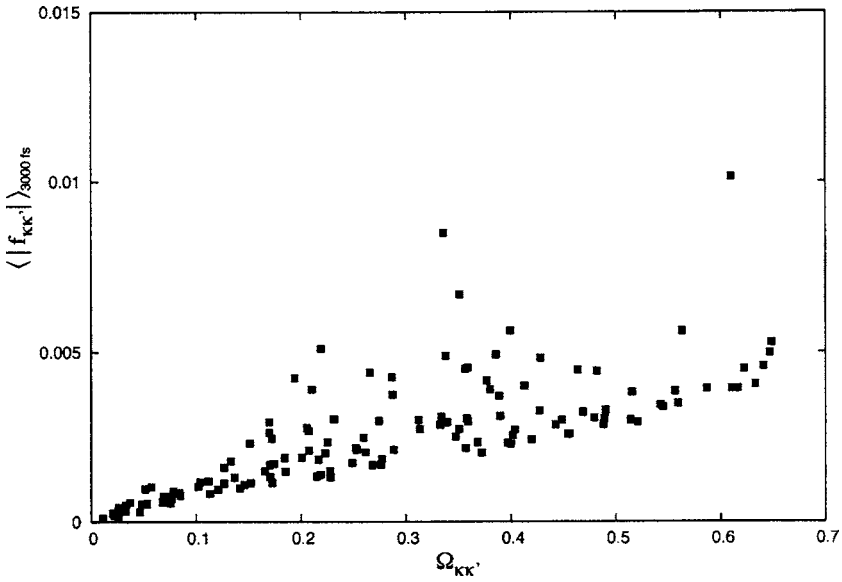

FIG. 9. The average over 3000 fs of $|f_{\kappa\kappa'}|$ vs resonance overlap for a representative selection of resonance pairs. This shows further connection between resonance overlap and controllability.

back to the Q subspace. Such "reverse flows," which are the hallmark of overlapping resonances,[28] are observed to occur in all the multiresonance optimized cases at $t > \sim 50$ fs. An example is given in Fig. 7 where the maximized (minimized) curves are shown for optimization times of 50 and 65 fs. Notice the recrossing hump in the maximized curve of the 65 fs optimization that is absent in the 50 fs curve.

As mentioned above, control between two states is, in principle, determined not only by the overlap of the two resonances but also by any common overlap of the two resonances with a third resonance. In practice these distinctions are unnecessary because, typically, the overlap of two states scales like the overlap of the two states with a common third state. In other words, $A_{\kappa'\kappa}$ of Eq. (12) is a monotonically increasing function of $\Omega_{\kappa'\kappa}$ of Eq. (11). This behavior is exactly what is observed in Fig. 8, where a plot of $A_{\kappa'\kappa}$ vs $\Omega_{\kappa'\kappa}$ is shown for representative pairs of basis states. We see that, although there is some noise, there is a clear monotonic trend in the data.

Finally, we display in Fig. 9 the average magnitude of $f_{\kappa'\kappa}$ over the time interval Δ, i.e.,

$$\langle f_{\kappa'\kappa}(t) \rangle_\Delta = \frac{1}{\Delta} \int_0^\Delta dt |f_{\kappa'\kappa}(t)|, \tag{17}$$

for $\Delta = 3000$ fs vs $\Omega_{\kappa\kappa'}$. These data show the strong connection between the overlap of the resonances and the average value of the interference contribution $f_{\kappa'\kappa}$.

IV. CONCLUSION

This paper examines the quantum control of IC in 24-mode pyrazine. The results are extremely encouraging: it is possible to almost completely suppress the process over time scales of ~50–100 fs, well in excess of the natural process (~20 fs), or to accelerate it to be over in less than 5 fs. The results are much more impressive than those in the limited reduced dimensionality ones, presumably because of the increased degree of overlap between bound state resonances existing in the correct picture of 24-mode pyrazine. It also suggests similar possible control in reasonably sized molecules.

The approach proposed here is *active* in that it does not rely on the chance occurrence of "extreme motion" states[26,29,30] that are primarily S_2 in character. Instead, the method relies entirely on the use of many overlapping-interfering resonances via the prepared initial state.

[1] M. Shapiro and P. Brumer, *Principles of the Quantum Control of Molecular Processes* (Wiley, New York, 2003).
[2] S. A. Rice and M. Zhao, *Optical Control of Molecular Dynamics* (Wiley, New York, 2000).
[3] K. Bergmann, H. Theuer, and B. W. Shore, Rev. Mod. Phys. **70**, 1003 (1998) and references therein.
[4] P. Král, J. Fiurášek, and M. Shapiro, Phys. Rev. A **64**, 023414 (2001); P. Král, Z. Amitay, and M. Shapiro, Phys. Rev. Lett. **89**, 063002 (2002).
[5] C. Daniel, J. Full, L. Gonzalez, C. Lupulescu, J. Manz, A. Merli, S. Vajda, and L. Wöste, Science **299**, 536 (2003).
[6] K. Hoki and P. Brumer, Phys. Rev. Lett. **95**, 168305 (2005).
[7] M. Spanner and P. Brumer, Phys. Rev. A **73**, 023809 (2006); **73**, 023810 (2006).
[8] E. Frishman and M. Shapiro, Phys. Rev. Lett. **87**, 253001 (2001).
[9] P. S. Christopher, M. Shapiro, and P. Brumer, J. Chem. Phys. **123**, 064313 (2005).
[10] E. S. Medvedev and V. I. Osherov, *Radiationless Transitions in Polyatomic Molecules* (Springer-Verlag, Berlin, 1995).
[11] K. F. Freed, Top. Appl. Phys. **15**, 23 (1976).
[12] J. Michl and V. Bonacic-Koutecky, *Electronic Aspects of Organic Photochemistry* (Wiley, New York, 1990).
[13] R. W. Schoenlein, L. A. Peteanu, R. A. Mathies, and C. V. Shank, Science **254**, 412 (1991).
[14] J. Jortner and M. A. Ratner, *Molecular Electronics* (Osney Mead, Oxford/Blackwell Science, Malden, MA, 1997).
[15] M. Klessinger and J. Michl, *Excited States and Photochemistry of Organic Molecules* (VCH, New York, 1990).
[16] V. Stert, P. Farmanara, and W. Radloff, J. Chem. Phys. **112**, 4460 (2000).
[17] A. Raab, G. A. Worth, H.-D. Meyer, and L. S. Cederbaum, J. Chem. Phys. **110**, 936 (1999).
[18] M. Seel and W. Domcke, J. Chem. Phys. **95**, 7806 (1991).
[19] G. Stock and W. Domcke, J. Chem. Phys. **97**, 12466 (1993).
[20] A. L. Sobolweski, C. Woywod, and W. Domcke, J. Chem. Phys. **98**, 5627 (1993).
[21] J. Kommandeur, W. A. Majewski, W. L. Meerts, and D. W. Pratt, Annu. Rev. Phys. Chem. **38**, 433 (1987).
[22] I. Burghardt, J. T. Hynes, E. Gindensperger, and L. S. Cederbaum, Phys. Scr. **73**, C42 (2006).

[23] D. Gerbasi, P. Christopher, A. Sanz, M. Shapiro, and P. Brumer, J. Chem. Phys. (in press).
[24] P. S. Christopher, M. Shapiro, and P. Brumer, J. Chem. Phys. **124**, 184107 (2006).
[25] A. Ferretti, A. Lami, and G. Villani, Chem. Phys. **196**, 447 (1995).
[26] M. Sukharev and T. Seideman, Phys. Rev. Lett. **93**, 093004 (2004).
[27] M. Thoss, W. H. Miller, and G. Stock, J. Chem. Phys. **112**, 10282 (2000).
[28] M. Shapiro, J. Phys. Chem. **102**, 9570 (1998).
[29] M. Shapiro and M. S. Child, J. Chem. Phys. **76**, 6176 (1982).
[30] G. Hose and H. S. Taylor, Chem. Phys. **84**, 375 (1984).